

A Theoretical Study of Dinitrogen Activation by Vanadium(II) and Vanadium(III): *Ab Initio* Calculations on Various Model Compounds

Nazzareno Re, Marzio Rosi, and Antonio Sgamellotti*

Dipartimento di Chimica, Università di Perugia, Via Elce di Sotto 8, I-06100 Perugia, Italy

Carlo Floriani and Euro Solari

Section de Chimie, Université de Lausanne, Place du Château 3, CH-1005, Lausanne, Switzerland

Received July 8, 1993[⊗]

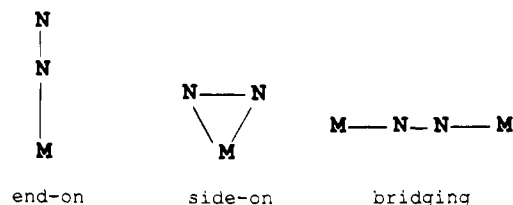
Ab initio RHF and CI calculations have been carried out on the $[\text{H}_3\text{VN}_2\text{VH}_3(\mu\text{-Na})]^-$, $[\text{H}_3\text{VN}_2\text{VH}_3]^-$, $[\text{H}_3\text{VN}_2\text{VH}_3]$, and $[\text{H}_3\text{VN}_2\text{VH}_3]^{2-}$ complexes and related fragments in order to study the energetics and the mechanism of dinuclear dinitrogen activation by vanadium(II) and vanadium(III). Analogous calculations have been performed also on the $[\text{H}_3\text{VN}_2]$, $[\text{H}_3\text{VN}_2]^-$, and $[\text{H}_3\text{VN}_2\text{Na}]$ complexes to compare mononuclear and dinuclear activation. Various energy gradient optimizations have been performed on the complexes and the various fragments, followed by MRCI calculations on the stationary structures. The results indicate that in the dinuclear complexes dinitrogen is poorly to strongly activated through mechanisms which depend on the presence of the alkali atom, the net charge, and the spin multiplicity of the considered state, while in the mononuclear complexes dinitrogen is always poorly activated.

Introduction

Dinitrogen coordination by metal complexes has received much interest for a long time as it can be considered the first step in the dinitrogen fixation process.^{1–4} The huge stability of the nitrogen molecule has always made its activation and fixation to useful products a difficult problem. From an experimental point of view several kind of dinitrogen transition metal complexes have been observed differing both in their nuclearity and in the bonding mode of the N_2 molecule.^{5–7} In particular, we recall the end-on and side-on bonding in mononuclear complexes and the terminal bridge bonding with a metal atom on each nitrogen atom in the dinuclear complexes; see Chart 1.

Although several *ab initio* investigations have been performed on mononuclear metal–dinitrogen complexes,^{8–18} only few^{19,24–28} and mainly semiempirical calculations^{8,20,21} have been performed on dinuclear complexes.

Chart 1



The binding of dinitrogen to a nucleophilic metallic fragment in a mononuclear complex is usually qualitatively described by the Chatt–Dewar–Duncanson model²² with σ donation from the dinitrogen lone pair to an empty orbital of the metal atom and π back-donation from an occupied metal orbital to the empty dinitrogen π^* orbital. When a dinuclear metal–dinitrogen complex is considered, the four-center M–N–N–M π interactions have been described more in detail through the simple qualitative molecular orbital scheme reported in Figure 1.²³ There are actually two sets of these four-center molecular orbitals which are obtained by linear combinations of respec-

* Abstract published in *Advance ACS Abstracts*, August 1, 1994.

- (1) Allen, A. D.; Harris, R. O.; Loescher, B. R.; Stevens, J. R.; Whiteley, R. N. *Chem. Rev.* **1973**, *73*, 13.
- (2) Olivé, G. H.; Olivé, S. *Coordination and Catalysis*; Verlag Chemie: Weinheim, Germany, 1977.
- (3) Chatt, J.; Dilworth, J. R.; Richards, R. L. *Chem. Rev.* **1978**, *78*, 859.
- (4) da Camara Pina, C. L. M.; Richard, R. L., Eds. *New Trends in the Chemistry of Nitrogen Fixation*; Academic Press: London, 1980.
- (5) Henderson, R. A.; Leigh, G. J.; Pickett, C. J. *Adv. Inorg. Chem. Radiochem.* **1983**, *27*, 197.
- (6) Pez, G. P.; Appgar, P.; Crissey, R. K. *J. Am. Chem. Soc.* **1982**, *104*, 482.
- (7) Jeffery, J.; Lappert, M. F.; Riley, P. I. *J. Organomet. Chem.* **1979**, *181*, 25.
- (8) Pelikan, P.; Boca, L. *Coord. Chem. Rev.* **1984**, *55*, 55.
- (9) Lauher, J. H.; Hoffmann, R. *J. Am. Chem. Soc.* **1976**, *98*, 1729.
- (10) Veillard, H. *Nouv. J. Chim.* **1978**, *2*, 215.
- (11) Murrel, J. N.; Al-Derzi, A.; Leigh, G. L.; Guest, M. F. *J. Chem. Soc., Dalton Trans.* **1980**, 1425.
- (12) Ondrechen, M. J.; Ratner, M. A.; Ellis, D. E. *J. Am. Chem. Soc.* **1981**, *103*, 1656.
- (13) Hori, K.; Asai, Y.; Yamabe, T. *Inorg. Chem.* **1983**, *22*, 3218.
- (14) Siegbahn, P. E. M.; Blomberg, M. R. A. *Chem. Phys.* **1984**, *87*, 189.
- (15) Sakaki, S.; Morokuma, K.; Ohkubo, K. *J. Am. Chem. Soc.* **1985**, *107*, 2686.
- (16) Sakaki, S.; Ohkubo, K. *J. Phys. Chem.* **1989**, *93*, 5655.

- (17) Rosi, M.; Sgamellotti, A.; Tarantelli, F.; Floriani, C.; Cederbaum, L. S. *J. Chem. Soc., Dalton Trans.* **1989**, 33.
- (18) Ciullo, G.; Rosi, M.; Sgamellotti, A.; Floriani, C. *Chem. Phys. Lett.* **1991**, *185*, 522.
- (19) Rappé, A. K. *Inorg. Chem.* **1984**, *23*, 995; **1986**, *25*, 4686.
- (20) Powell, C. B.; Hall, M. B. *Inorg. Chem.* **1984**, *23*, 4619.
- (21) Goldberg, K. I.; Hoffmann, D. F.; Hoffmann, R. *Inorg. Chem.* **1982**, *21*, 3863.
- (22) Dewar, M. J. S. *Bull. Soc. Chim. Fr.* **1951**, *18c*, 71. Chatt, J.; Duncanson, J. A. *J. Chem. Soc.* **1953**, 2939.
- (23) Chatt, J.; Fay, R. C.; Richards, R. L. *J. Chem. Soc. A* **1971**, 2399. Treitel, J. M.; Flood, M. T.; March, R. E.; Gray, H. B. *J. Am. Chem. Soc.* **1969**, *91*, 6512. Sellmann, D. *Angew. Chem.* **1974**, *13*, 639.
- (24) Bauschlicher, C. W., Jr.; Pettersson, L. G. M.; Siegbahn, P. E. M. *J. Chem. Phys.* **1987**, *87*, 2129.
- (25) Siegbahn, P. E. M. *Chem. Phys.* **1991**, *95*, 364.
- (26) Blomberg, M. R. A.; Siegbahn, P. E. M. *Chem. Phys. Lett.* **1991**, *179*, 524.
- (27) Fryzuk, M. D.; Haddad, T. S.; Mylvaganam, M.; McConville, D. H.; Rettig, S. J. *J. Am. Chem. Soc.* **1993**, *115*, 2782.
- (28) Blomberg, M. R. A.; Siegbahn, P. E. M. *J. Am. Chem. Soc.* **1993**, *115*, 6908.

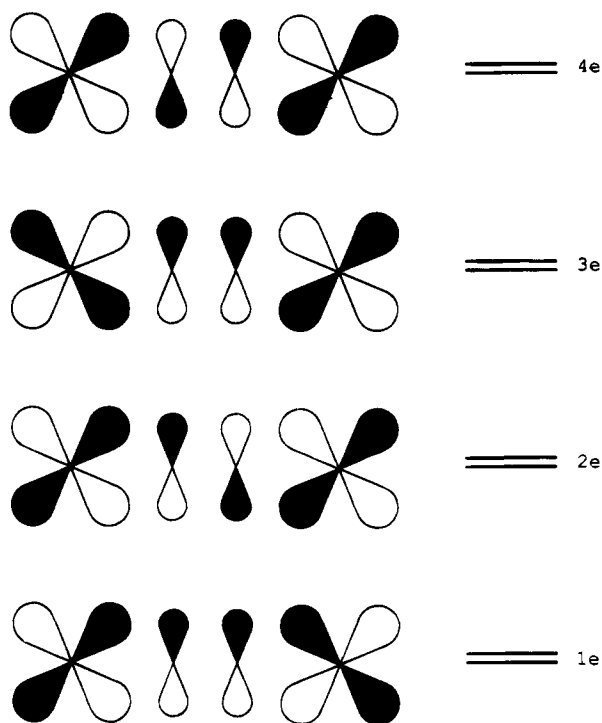


Figure 1. Schematic representation of orbital interactions involved in the end-on bonded dinuclear dinitrogen complexes.

tively Md_{xy} , Np_x or Md_{yz} , Np_z orbitals (with the y -axis determined by the σ bond direction). As overall result, we have four doubly degenerate energy levels whose energies increase with increasing nodal number of the molecular orbitals and which are designated as 1e, 2e, 3e, and 4e. The scheme is completed by the δ bond type orbitals built by the bonding and antibonding combinations of d_{xy} and $d_{x^2-y^2}$ orbitals which contribute practically nothing to the bonding because of the high M—M distance. The relative strength of the M—N and N—N bonds depends mainly on the occupancy number of these levels by the d electrons of the metals and the π electrons of N_2 . Such strength considerations must take into account (i) the N—N bonding character of the 1e and 3e orbitals and the N—N antibonding character of the 2e and 4e orbitals, (ii) the M—N bonding character of 1e and 2e orbitals and the M—N antibonding character of 3e and 4e orbitals, and (iii) the mainly dinitrogen character of the 1e and 4e orbitals and metal character of the 2e and 3e orbitals. Most of the theoretical calculations performed on dinuclear N_2 complexes^{19,20,24–28} have been interpreted in terms of the 1e–4e levels occupancy and also in terms of the relative metal–nitrogen composition of the corresponding orbitals.

Activation of dinitrogen by bridging end-on coordination in dinuclear systems has been studied for a long time^{29–34} and is particularly efficient for early transition metals. Dinitrogen activation is commonly thought to be gauged by a lengthening in N—N bond distance with respect to free N_2 (1.10 Å). Indeed, the lengthening of the N—N bond distance is usually related to

a reduction of the N—N bond order by direct comparison with the values for an N—N double bond in azomethane (1.24 Å) and N—N single bond in hydrazine (1.47 Å). However, recent experimental studies on dinitrogen coordination in dinuclear systems^{34,35} have shown that lengthening of the N—N distance is not always strictly related to its activation, very elongated N_2 molecules being sometimes inert to protonation.³⁶

This theoretical study is addressed to very recent experimental results reported in vanadium dinitrogen chemistry.³⁷ Such an investigation led to the isolation and full characterization of two dinuclear V(II)–V(II) and V(II)–V(III) complexes: $[Mes_3V-N_2-VMes_3(\mu-Na)]-[Na(diglyme)_2]^+$, **1**, and $[Mes_3V-N_2-VMes_3]^- [K(diglyme)_2]^+$, **2** [Mes = 2,4,6-(CH₃)₃C₆H₂; diglyme = CH₃OCH₂CH₂OCH₂CH₂OCH₃]. Complexes **1** and **2** showed some peculiar and unique characteristics, as follows: (i) magnetic moments correspond to two unpaired electrons in **1** and one unpaired electron in **2**; (ii) protonation of **1** and **2** led to the evolution of N_2H_4 and NH_3 , proving that dinitrogen is present in reduced form. The origin of **1** and **2** has been proposed to occur very likely as reported in the scheme of ref 37 along with their structures.

Those results prompted us to investigate the following model compounds where the mesityl residue has been replaced by a hydrido ligand, though the bonding connectivity remains the same: $[H_3V-N_2-VH_3]$, **3**; $[H_3V-N_2-VH_3]^-$, **4**; $[H_3V-N_2-VH_3]^{2-}$, **5**; $[H_3V-N_2-VH_3(\mu-Na)]^-$, **6**; $[H_3V-N_2]$, **7**; $[H_3V-N_2]^-$, **8**; $[H_3V-N_2Na]$, **9**.

Complexes **4–6** are model compounds very close to isolated and characterized species, while **7–9** should be considered as plausible precursors of the isolated species.

Computational Details

Basis Set. The s , p basis for vanadium was taken from the (12s6p4d) set of ref 38 with the addition of two basis functions to describe the 4p orbital³⁹ and the deletion of the outermost s function, while the V d basis was the reoptimized (5d) set of ref 40, contracted (4/1). This leads to an (11s8p5d) primitive basis for vanadium, contracted (8s6p2d). A double- ζ expansion was used for all the other ligand atoms, with a (4s/2s) basis for hydrogen⁴¹ and a (9s5p/4s2p) contraction for nitrogen.⁴¹

Methods. The calculations have been performed at two levels of accuracy. An LCAO–SCF–MO scheme has been employed to derive ground-state energies and wave functions for all the investigated structures of the system and to perform the various geometry optimizations and transition state calculations. Multiple-reference configuration interaction (MRCI) calculations, including all the configurations with a CI expansion coefficient greater than 0.05, were subsequently performed on some of the stationary points determined at the SCF level. These calculations have been performed with the direct CI method.⁴² To reduce the size of the CI problem, the V 1s, 2s, and 2p core orbitals have been frozen in all the calculations. A Davidson correction⁴³ was added to correct for the effect of unlinked clusters in these CI calculations.

All computations were performed by using the GAMESS program package,⁴⁴ implemented on IBM RS 6000 workstations.

(29) Sanner, R. D.; Manriquez, J. M.; Marsh, R. E.; Bercaw, J. E. *J. Am. Chem. Soc.* **1976**, *98*, 8351.

(30) Sanner, R. D.; Duggan, D. M.; McKenzie, T. C.; Marsh, R. E.; Bercaw, J. E. *J. Am. Chem. Soc.* **1976**, *98*, 8358.

(31) Schrock, R. R.; Wesolek, M.; Liu, A. H.; Wallace, K. C.; Dewan, J. C. *Inorg. Chem.* **1988**, *27*, 2050.

(32) Fryzuk, M. D.; Haddad, T. S.; Rettig, S. J. *J. Am. Chem. Soc.* **1990**, *112*, 8185.

(33) Duchateau, R.; Gambarotta, S.; Beydoun, N.; Bensimon, C. *J. Am. Chem. Soc.* **1991**, *113*, 8986.

(34) Beydoun, N.; Duchateau, R.; Gambarotta, S. *J. Chem. Soc., Chem. Commun.* **1992**, 244.

(35) Leigh, G. J. *Acc. Chem. Res.* **1992**, *25*, 177.

(36) Buijink, J.-K. F.; Meetsma, A.; Teuben, J. H. *Organometallics* **1993**, *12*, 2004.

(37) Ferguson, R.; Solari, E.; Floriani, C.; Chiesi-Villa, A.; Rizzoli, C. *Angew. Chem., Int. Ed. Engl.* **1993**, *32*, 396 and unpublished results.

(38) Ross, R.; Veillard, A.; Vinot, G. *Theor. Chim. Acta* **1971**, *20*, 1.

(39) Hood, D. M.; Pitzer, R. M.; Schaeffer, H. F., III. *J. Chem. Phys.* **1979**, *71*, 705.

(40) Rappé, A. K.; Smedley, T. A.; Goddard, W. A., III. *J. Phys. Chem.* **1981**, *85*, 2607.

(41) Dunning, T. H., Jr. *J. Chem. Phys.* **1970**, *53*, 2823.

(42) Saunders, V. R.; Van Lenthe, J. H. *Mol. Phys.* **1983**, *48*, 923.

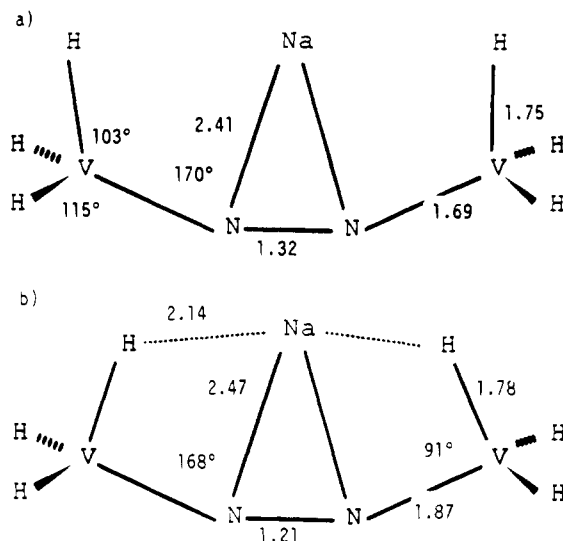
(43) Davidson, E. R. In *The World of Quantum Chemistry*; Daudel, R., Pullman, B., Eds.; Reidel: Dordrecht, The Netherlands, 1974.

(44) Guest, M. F.; Sherwood, P. GAMESS User Manual. Daresbury Technical Memorandum; Daresbury Laboratory, 1991.

Table 1. Total SCF and CI Energies (hartree) for the $[\text{H}_3\text{VN}_2(\text{Na})\text{VH}_3]^-$ Complex in the Lowest Singlet and Triplet States and Its VH_3^- , N_2 , and Na^+ Fragments^a

	SCF	CI
$[\text{H}_3\text{VN}_2(\text{Na})\text{VH}_3]^- (^1\text{A}_1)$	-2158.2884	-2159.0592
$[\text{H}_3\text{VN}_2(\text{Na})\text{VH}_3]^- (^3\text{B}_2)$	-2158.3048	-2159.1408
$\text{VH}_3^- (^4\text{A}'_1)$	-944.3124	-944.5501
$\text{N}_2 (^1\Sigma_g)$	-108.8481	-109.1215
$\text{Na}^+ (^1\text{S})$	-160.6737	-160.6747

^a In the same geometry as that of the $[\text{H}_3\text{VN}_2(\text{Na})\text{VH}_3]^- (^3\text{B}_2)$ complex.

**Figure 2.** Optimized geometries of the $[\text{H}_3\text{VN}_2\text{VH}_3(\mu\text{-Na})]^-$ complex in the (a) $^3\text{B}_2$ and (b) $^1\text{A}_1$ states.

Geometry and Geometry Optimization. In all the SCF calculations we have optimized all the geometrical parameters with the only exception of the VH_3 dihedral angle, fixed at 120° . The coordinate system has been chosen so that the z axis is the main symmetry axis. In the binuclear complexes this choice corresponds to the y axis parallel to the $\text{N}-\text{N}$ direction. All the geometry optimizations have been performed using the quasi-Newton procedure available in the GAMESS package.

Results and Discussion

Dinuclear Complexes. Calculations were first performed on the $[\text{H}_3\text{VN}_2\text{VH}_3(\mu\text{-Na})]^-$ complex. SCF geometry optimization of the lowest singlet and triplet states leads to the total energies and the geometries reported in Table 1 and Figure 2, respectively. In Table 1 we report also the CI energies obtained by performing direct CI calculations on the two optimized structures. We see that at the more accurate CI level the ground state is a triplet, $^3\text{B}_2$, with the first excited state, $^1\text{A}_1$, 49 kcal mol^{-1} higher in energy. This agrees with the experimentally observed magnetic character of complex **1** as a triplet ground state has been observed with a magnetic moment of $1.69 \mu_B$ per vanadium at 293 K (two unpaired electrons per dimer). The short $\text{V}-\text{N}$ bond length (1.68 Å) and the long $\text{N}-\text{N}$ bond length (1.32 Å) indicate a very perturbed dinitrogen moiety.

We have then considered the dinuclear vanadium nitrogen complex without the alkali metal, performing SCF geometry optimization of $[\text{H}_3\text{VN}_2\text{VH}_3]^-$ in the doublet and quartet states and evaluating the correlation energy through CI calculations on the optimized structures. We have also performed analogous calculations on $[\text{H}_3\text{VN}_2\text{VH}_3]$ and $[\text{H}_3\text{VN}_2\text{VH}_3]^{2-}$ in singlet and triplet states. We report the total energies in Table 2 and the main geometrical parameters of the optimized structures in Table 3. All these complexes have an optimized linear geometry, the

Table 2. Total SCF and CI Energies (hartree) for the $\text{H}_3\text{VN}_2\text{VH}_3$, $[\text{H}_3\text{VN}_2\text{VH}_3]^-$, and $[\text{H}_3\text{VN}_2\text{VH}_3]^{2-}$ Complexes in the Lowest Singlet and Triplet or Doublet and Quartet States (According to the Even or Odd Number of Electrons)

	SCF	CI
$\text{H}_3\text{VN}_2\text{VH}_3 (^3\text{B}_2)$	-1997.2460	-1997.9876
$\text{H}_3\text{VN}_2\text{VH}_3 (^1\text{A}_1)$	-1997.2378	-1997.9715
$[\text{H}_3\text{VN}_2\text{VH}_3]^- (^4\text{A}_1)$	-1997.3970	-1998.2138
$[\text{H}_3\text{VN}_2\text{VH}_3]^- (^2\text{B}_1)$	-1997.3132	-1998.2093
$[\text{H}_3\text{VN}_2\text{VH}_3]^{2-} (^3\text{B}_2)$	-1997.2987	-1998.1387
$[\text{H}_3\text{VN}_2\text{VH}_3]^{2-} (^1\text{A}_1)$	-1997.2753	-1998.0407

Table 3. Main Geometrical Parameters for the Optimized Structures of $\text{H}_3\text{VN}_2\text{VH}_3$, $[\text{H}_3\text{VN}_2\text{VH}_3]^-$, and $[\text{H}_3\text{VN}_2\text{VH}_3]^{2-}$ Complexes in the Ground and First Excited States^a

	N-N	V-N	V-H	$\angle\text{NVH}$
$[\text{H}_3\text{VN}_2\text{VH}_3] (^3\text{B}_1)$	1.19	1.85	1.63	111.7
$[\text{H}_3\text{VN}_2\text{VH}_3] (^1\text{A}_1)$	1.21	1.82	1.63	104.1
$[\text{H}_3\text{VN}_2\text{VH}_3]^- (^4\text{A}_1)$	1.24	1.77	1.68	115.5
$[\text{H}_3\text{VN}_2\text{VH}_3]^- (^2\text{B}_1)$	1.22	1.72	1.70	106.4
$[\text{H}_3\text{VN}_2\text{VH}_3]^{2-} (^3\text{B}_2)$	1.32	1.67	1.77	115.2
$[\text{H}_3\text{VN}_2\text{VH}_3]^{2-} (^1\text{A}_1)$	1.21	1.89	1.78	112.1

^a Bond lengths are in angstroms, and angles in degrees.

distortion observed in $[\text{H}_3\text{VN}_2\text{VH}_3(\mu\text{-Na})]^-$ being prevented by the absence of the alkali ion.

From Table 2 we see that the $[\text{H}_3\text{VN}_2\text{VH}_3]^-$ complex, in the $^4\text{A}_1$ state, is the most stable one both at the SCF and CI level, while the $[\text{H}_3\text{VN}_2\text{VH}_3]$ complex is far higher in energy and will not be discussed.

Considering first of all the $[\text{H}_3\text{VN}_2\text{VH}_3]^-$ complex, we see that the calculated ground state at the CI level is an $^4\text{A}_1$, although the first excited state is a $^2\text{B}_1$ only 3 kcal mol^{-1} higher in energy. However, taking into account (i) that the error due to the correlation energy, not completely corrected by a CI calculation based on the SCF wave function, favors the high-spin configuration and (ii) that there is a difference between the real complex **2** and our model, our calculations cannot provide a definitive assignment of the experimental ground state. The observed magnetic moment of **2**, $1.83 \mu_B$ at 293 K per bimetallic unit, indicates a doublet ground state, so that we discuss the $^2\text{B}_1$ wave function as the ground state. For this V(II)-V(III) complex we find a less perturbed dinitrogen moiety than that found for the V(II)-V(II) $[\text{H}_3\text{VN}_2\text{VH}_3(\mu\text{-Na})]^-$ and $[\text{H}_3\text{VN}_2\text{VH}_3]^{2-}$ species. Indeed, from Table 3 we see that the main difference in the optimized geometry is the slightly longer $\text{V}-\text{N}$ bond length (1.72 Å) and the shorter $\text{N}-\text{N}$ bond length (1.22 Å).

Finally, the $[\text{H}_3\text{VN}_2\text{VH}_3]^{2-}$ complex can be regarded as derived from the $[\text{H}_3\text{VN}_2\text{VH}_3(\mu\text{-Na})]^-$ pulling off the Na^+ ion. Indeed, from Table 2 we see that the triplet state is lower than the singlet one by almost the same energy amount found for the $[\text{H}_3\text{VN}_2\text{VH}_3(\mu\text{-Na})]^-$ complex, while from Table 3 we note the strong similarity of the common geometrical parameters ($\text{V}-\text{N}$, $\text{N}-\text{N}$, and $\text{V}-\text{H}$ bond lengths and $\angle\text{NVH}$ angle) for the two complexes in states of the same spin symmetry, with a parallel trend when we pass from the singlet to the triplet states in both cases. The comparison between the two complexes may help to elucidate the role of the alkali ion. The binding energy of the Na^+ ion is easily evaluated as 212 and 202 kcal mol^{-1} at the SCF level, respectively for the triplet and the singlet state. The high value of this binding energy must not surprise as it corresponds to the electrostatic interaction between the Na^+ ion and the $[\text{H}_3\text{VN}_2\text{VH}_3]^{2-}$ dianion, as supported by the fact that repeating the calculation on the $[\text{H}_3\text{VN}_2\text{VH}_3]^{2-}$ complex in the geometry of the $[\text{H}_3\text{VN}_2\text{VH}_3(\mu\text{-Na})]^- ^3\text{B}_2$ optimized structure with a +1 point charge replacing the Na^+ ion we obtain a stabilization energy of 190 kcal mol^{-1} and a bonding situation

essentially identical to that found for the whole $[\text{H}_3\text{VN}_2\text{VH}_3(\mu\text{-Na})]^-$ $^3\text{B}_2$ complex.

The main results which can be drawn from these calculations is that all the considered complexes can be classified in two distinct classes which differ both in the spin state and in the degree of perturbation of the N_2 unit. The $[\text{H}_3\text{VN}_2\text{VH}_3(\mu\text{-Na})]^-$ and $[\text{H}_3\text{VN}_2\text{VH}_3]^{2-}$ complexes have a more perturbed N_2 unit ($\text{N}-\text{N} = 1.32 \text{ \AA}$) and a high spin state ($S = 1$), while the $[\text{H}_3\text{VN}_2\text{VH}_3]^-$ complex has a less perturbed N_2 unit ($\text{N}-\text{N} = 1.22 \text{ \AA}$) and a low spin state ($S = 1/2$). An explanation of these differences can be made on the basis of the different occupancy number of the four-center molecular orbitals scheme of Figure 1 and will be considered in detail in the next paragraph.

In a recent paper²⁸ Siegbahn et al. performed *ab initio* calculations on analogous dinuclear systems but with ligand-free metals. Their results also led to two different kind of states, one with a more perturbed N_2 unit ($\text{N}-\text{N}$ about 1.3 \AA) and one with a less perturbed N_2 unit ($\text{N}-\text{N}$ about 1.2 \AA), but in that case the most perturbed state has a lower spin. Although they interpreted their results with the same four-center molecular orbitals scheme, a direct comparison is not possible both because they considered different metals and because they did not account for ligand effects. However, the different results obtained by us for the spins of the two differently perturbed states are essentially due to the possible occupation of the nonbonding symmetric and antisymmetric combinations of the d_δ orbitals²³ which were not considered in ref 28.

Bonding Mode and Molecular Orbital Analysis. In an effort to localize the factors determining the differences between the two classes of complexes identified by our calculations, we performed an accurate analysis of the frontier molecular orbitals and therefore of the electronic structure of all the considered complexes.

We begin to analyze the electronic structure of the $[\text{H}_3\text{VN}_2\text{VH}_3(\mu\text{-Na})]^-$ complex. Starting with the $^3\text{B}_2$ ground state, several interesting features come out from its geometrical structure reported in Figure 2a: (i) There is the very short V-N bond length (1.69 \AA) and the long N-N one (1.32 \AA), fairly close to the experimental values for complex 1 (1.76 and 1.28 \AA), which indicate bond orders much higher than one and lower than three, respectively. (ii) There is an overall VNNV structure close to the linear geometry ($\angle\text{VNN} = 170^\circ$). (iii) There is a relatively short distance between the Na atom and the two hydrogen atoms lying in the plane of the molecule (2.39 \AA) which indicates a Na-H interaction. Such effect is also indicated by the optimized $\angle\text{NVH}$ angles which have a smaller value (103°) for the two interacting hydrogens than that for the other four hydrogens (115°). In order to quantify the energy of the Na-H interaction we have repeated the calculation on the $[\text{H}_3\text{VN}_2\text{VH}_3(\mu\text{-Na})]^-$ complex in a geometry differing from the optimized one only for a 180° rotation of the dihedral $\angle\text{NVH}$ angles, obtaining an energy value 21 kcal mol^{-1} higher. Assuming that the only difference in the electronic structure for the two geometries is the absence of the two Na-H interactions, we estimate an energy for each interaction of about $10.5 \text{ kcal mol}^{-1}$. (iv) There is an intermediate Na-N distance (2.41 \AA) which indicates a not-negligible contact between the sodium and the two nitrogens and hence an ion pair interaction with a noncovalent character of the Na-N bond itself. This latter point is confirmed by the analysis of the electronic structure discussed below.

A better interpretation of the metal-nitrogen bonding requires the analysis of the bonding pictures of the complexes. A more detailed and physically meaningful analysis of the molecular orbitals (MOs) of $[\text{H}_3\text{VN}_2\text{VH}_3(\mu\text{-Na})]^-$ may be performed in

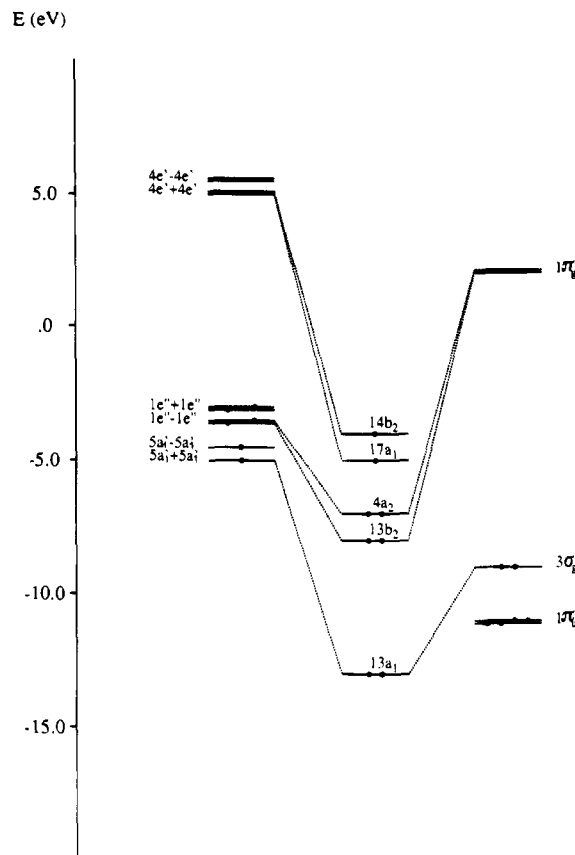


Figure 3. Molecular orbital diagram for the $[\text{H}_3\text{VN}_2\text{VH}_3(\mu\text{-Na})]^-$ complex in the $^3\text{B}_2$ state.

terms of orbital interactions between preformed fragments. Assuming the $[\text{H}_3\text{VN}_2\text{VH}_3(\mu\text{-Na})]^-$ complex as composed of a $[\text{H}_3\text{VN}_2\text{VH}_3]^{2-}$ unit and a Na^+ ion—as we will justify below—we can identify as one N_2 molecule and two VH_3^- species as the interacting fragments. In Figure 3 we show a diagram depicting the MOs for the two VH_3^- metallic fragments interacting with the MOs of the bridging N_2 molecule to reproduce the energy levels of the upper valence region of the $[\text{H}_3\text{VN}_2\text{VH}_3(\mu\text{-Na})]^-$ complex. The VH_3^- metallic fragment has been considered in its SCF optimized structure in the lowest $^4\text{A}'_1$ state. This structure corresponds to a planar geometry with D_{3h} symmetry, and its higher MOs are reported in Figure 4. The highest orbitals of VH_3^- in the lowest $^4\text{A}'_1$ state are the doubly occupied $4a'_1$ and $3e'$, which are involved in the σ V-H bonding, and the singly occupied $5a'_1$ and $1e''$, which are essentially pure d_{z^2} and d_{xz} , d_{yz} metal orbitals, respectively. The lowest unoccupied orbital is the doubly degenerate $4e'$, which corresponds essentially to d_{xy} and $d_{x^2-y^2}$ metal orbitals.

Actually in Figure 3 we report the energy levels for the two VH_3^- fragments at the same distance observed in the whole complex ($\approx 5 \text{ \AA}$); due to extremely small interactions these levels consist in almost degenerate symmetric and antisymmetric combinations of those for the single fragment. In Figure 3 we report also the main valence orbitals of the N_2 molecule, i.e. the doubly occupied $3\sigma_g$, the doubly degenerate quadruply occupied $1\pi_u$, and the empty $1\pi_g$ MO.

The main bonding orbitals between vanadium atoms and dinitrogen are the two highest occupied ones, $13b_2$ and $4a_2$, which correspond respectively to the overlap between the antisymmetric $3d_{xy} - 3d'_{xy}$ combination of vanadium orbitals and one of the two components of the virtual $1\pi_g$ orbital of N_2 (hereafter also denoted as π^*) and between the antisymmetric $3d_{yz} - 3d'_{yz}$ combination of vanadium orbitals and the other component of the virtual $1\pi_g$ orbital of N_2 . Therefore these

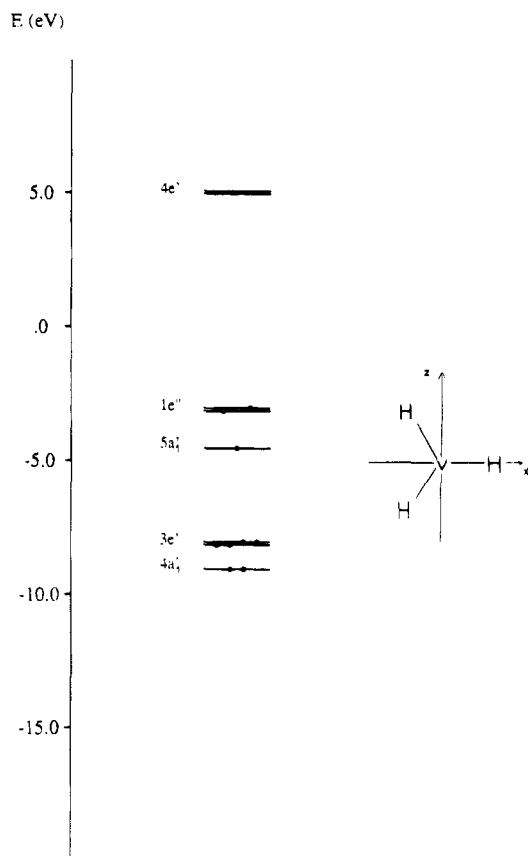


Figure 4. Molecular orbital diagram for the VH_3^- fragment in a planar geometry of D_{3h} symmetry.

two MOs describe π back-donation from vanadium to dinitrogen; it is worth noting that there is a double back-donation effect which could be interpreted as leading to a single bond between nitrogen in N_2 and a triple bond between vanadium and nitrogen. The two singly occupied orbitals, $14b_2$ and $17a_1$, are essentially symmetric combinations of pure $d_{x^2-z^2}$ and d_{xz} vanadium orbitals. σ donation is described by the MO $13a_1$, which corresponds to a weak overlap between the $3\sigma_g$ orbital of N_2 and a hybrid orbital of the two vanadium atoms formed mainly by $4s$, $3d_{y^2}$. The bonding analysis can be completed by discussing it in terms of the M—N—N—M molecular orbital scheme of Figure 1, accounting for the slight deformations due to the nonlinear geometry. First of all we note that the $13b_2$ and $4a_2$ MOs correspond to the $2e$ orbitals and show a relevant mixing of metal and dinitrogen orbitals. The lower $4b_1$ and $14a_1$ MOs correspond to the $1e$ orbitals. Their character is almost pure N_2 $1\pi_u$ for the former but is fairly stabilized by the symmetric $d_{yz} + d'_{yz}$ combination of metal orbitals for the latter (leading to a slight weakening of the N—N bond strength). This scheme is completed by identifying the two singly occupied orbitals with the $d_{x^2-z^2}$ and d_{xz} δ type orbitals. In this scheme the nonoccupancy of the N—N bonding $3e$ orbitals and the high metal—dinitrogen orbital mixing in the $2e$ orbitals enable us to predict a consistent reduction of the N—N bond order and an increase of the V—N one.

A Mulliken population analysis of the various complexes helps in understanding the bonding picture for the $[\text{H}_3\text{VN}_2\text{VH}_3-(\mu\text{-Na})]^-$ complex. In Table 4 we report the Mulliken atomic charges and the Mulliken population changes of the whole complex with respect to the VH_3^- , N_2 , and Na^+ fragments. First of all we see that the sodium atom bears a charge of about +0.50, which indicates its ionic character and supports the assumption of a Na^+ fragment. The two N atoms gain almost 1.3 electron charge units mainly localized on the $2p_x$ and $2p_z$

Table 4. Total Mulliken Atomic Charges, Spin Populations, and Mulliken Population Changes of Various Orbitals for the $[\text{H}_3\text{VN}_2(\text{Na})\text{VH}_3]^-$ (3B_2) Complex with Respect to the VH_3^- , N_2 , and Na^+ Fragments

	atomic charge	spin population	population change
V	+0.64	0.98	-0.50
V s			+0.17
V p		0.02	0.00
p_x			-0.02
p_y			+0.08
p_z		0.02	-0.06
V d		0.96	-0.37
$d_{x^2-z^2}$		0.31	+0.04
d_{y^2}		0.42	+0.15
d_{xy}			-0.28
d_{xz}			+0.07
d_{yz}		0.23	-0.30
N	-0.64	0.01	+0.64
N s			-0.11
p_x			+0.46
p_y			-0.20
p_z			+0.45
Na	+0.50	0.01	-0.50
Na s		0.01	-0.81
p_x			+0.03
p_y			+0.24
p_z			+0.04
H_1	-0.29		-0.10
H_2	-0.23		-0.15

orbitals (+0.46 and +0.45, respectively), i.e. on the $1\pi_g$ antibonding orbitals of the N_2 molecule; at the same time there is a strong decrease of the population of the d_{π} orbitals (-0.28 for the d_{xy} and -0.30 for the d_{yz}). This effect is directly related to π back-donation, and it has been observed in all the previous *ab initio* calculations on mononuclear metal—dinitrogen complexes but at a remarkably lesser extent, especially for the end-on coordination which directly compares with our dinuclear complexes.⁸⁻¹⁵ The σ donation, on the other hand, is reflected in the increase of the population of the vanadium $4s$ and d_{σ} orbitals (+0.17 and +0.19 electrons, respectively) and in the simultaneous decrease of the nitrogen s and p_y populations (0.11 and 0.20 e, respectively). Such effect is however much less relevant than the previous one.

Altogether, the results of the MO and Mulliken population analysis indicate a strong perturbation of the dinitrogen molecule, in good agreement with the experimental data, and suggest that π back-donation plays a predominant role with respect to σ donation.

It may be interesting to analyze also the lowest excited singlet state, 1A_1 , to point out the reasons of its differences with the triplet ground state. An accurate analysis of this 1A_1 state reveals many features in common with the triplet state but also some important differences. The optimized geometrical structure reported in Figure 2b shows the following relevant points with respect to the triplet ground state: (i) There is a longer V—N bond length (1.87 Å) and a shorter N—N bond length (1.21 Å), which indicate a significantly lower perturbation of N_2 . (ii) There is a shorter distance between the Na atom and the two hydrogen atoms lying in the plane of the molecule (2.14 Å). Such shortening implies an increase of the Na—H interaction. Repeating the calculation on the same complex in a geometry differing from the optimized one only for a 180° rotation of the dihedral NNVH angle, we obtain an energy value 37 kcal mol⁻¹ higher (cf. 21 kcal mol⁻¹ for the triplet case).

Other features of the singlet state come out from the analysis of the bonding picture and of the orbital interactions among preformed fragments. In Figure 5 we show a diagram depicting the MOs for the two VH_3^- metallic fragments interacting with

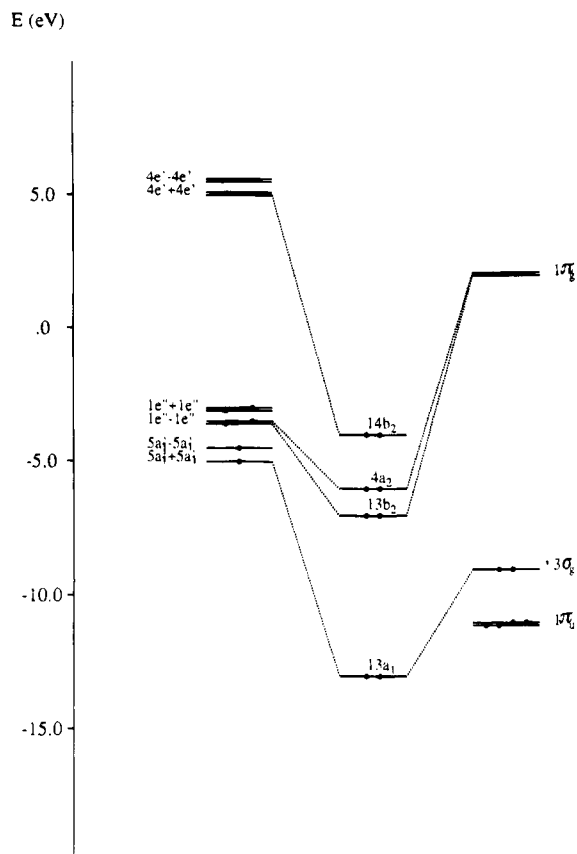


Figure 5. Molecular orbital diagram for the $[\text{H}_3\text{VN}_2\text{VH}_3(\mu\text{-Na})]^-$ complex in the $^1\text{A}_1$ state.

the MOs of the bridging N_2 molecule to reproduce the energy levels of the upper valence region of the singlet $[\text{H}_3\text{VN}_2\text{VH}_3(\mu\text{-Na})]^-$ complex. The VH_3^- metallic fragments have been considered in the same optimized planar geometry discussed above, whose MO structure is reported in Figure 4.

The main bonding orbitals between vanadium atoms and dinitrogen are still the $13b_2$ and $4a_2$, which correspond to the two antisymmetric $3d_{xy} - 3d'_{xy}$ and $3d_{yz} - 3d'_{yz}$ combinations of vanadium orbitals, respectively, only slightly mixed with the components of the virtual π^* orbital of N_2 . σ donation is described by the MO $13a_1$ which corresponds to a weak overlap between the $3\sigma_g$ orbital of N_2 and the $4s$ orbital of the two vanadium atoms. In terms of the M—N—N—M molecular orbital scheme, the $13b_2$ and $4a_2$ orbitals correspond to the $2e$ orbitals while the $1e$ orbitals are constituted by the $14a_1$ and $4b_1$ MOs, with a doubly occupied $14b_2$ orbital corresponding to a $d_{x^2-z^2}$ δ type orbital.

We can therefore conclude that the lowest excited state, $^1\text{A}_1$, corresponds essentially to the same configuration of the ground triplet state with the two unpaired electrons paired on a vanadium d orbital.

The results of this analysis of the singlet state indicate a lower perturbation of the dinitrogen molecule with respect to the triplet ground state.

We then consider the $[\text{H}_3\text{VN}_2\text{VH}_3]^-$ complex to point out why, for this V(II)-V(III) complex, we find an electronic structure slightly different from that found for the V(II)-V(II) $[\text{H}_3\text{VN}_2\text{VH}_3(\mu\text{-Na})]^-$ and $[\text{H}_3\text{VN}_2\text{VH}_3]^{2-}$ species. This difference can be interpreted from an analysis of the bonding scheme for the two states which follows from the Mulliken population reported in Table 5 and from the diagram of the higher energy levels with the related interactions between the VH_3^- and N_2 MOs reported in Figure 6. In particular, the analysis of the

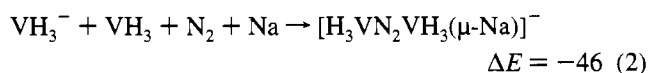
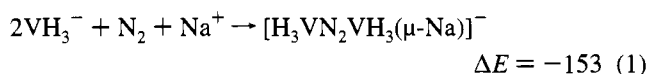
Table 5. Total Mulliken Atomic Charges, Spin Populations, and Mulliken Population Changes of Various Orbitals for the $[\text{H}_3\text{VN}_2\text{VH}_3]^-$ Complex in the (a) $^2\text{B}_1$ and (b) $^4\text{A}_1$ States with Respect to the VH_3^- and N_2 Fragments in the Same Geometry of the Corresponding Optimized Complex

	atomic charge	spin population	population change
(a) $^2\text{B}_1$ State			
V	+0.43	0.43	-0.29
V s			+0.45
V p			-0.03
p_x			-0.02
p_y			+0.02
p_z			-0.03
V d			-0.34
$d_{x^2-z^2}$			-0.07
d_{xy}		0.37	+0.41
d_{xz}		0.05	+0.03
d_{yz}			-0.40
N	-0.33	0.05	+0.33
N s			-0.07
p_x		0.05	+0.14
p_y			-0.24
p_z			+0.51
H_1	-0.21		-0.17
H_2	-0.20		-0.18
(b) $^4\text{A}_1$ State			
V	+0.58	1.13	-0.44
V s			+0.28
V p		0.05	-0.05
p_x			-0.01
p_y			+0.02
p_z		0.05	-0.06
V d		1.08	-0.42
$d_{x^2-z^2}$		0.11	-0.01
d_{xy}		0.62	+0.06
d_{xz}			-0.24
d_{yz}			+0.05
N	-0.52	0.36	-0.28
N s		0.35	+0.52
p_x			-0.09
p_y			+0.48
p_z		0.35	-0.15
H_1	-0.20		+0.30
H_2	-0.18		-0.18

molecular orbitals reveals that in both cases the main bonding orbitals are the two highest doubly occupied ones ($12b_2$ and $4a_2$), which correspond to the overlap of the two π^* N_2 orbitals with the antisymmetric $3d_{xy} - 3d'_{xy}$ and $3d_{yz} - 3d'_{yz}$ combinations of vanadium orbitals and describe π back-donation from vanadium to dinitrogen, and the lower $10a_1$, which corresponds to the overlap between the N_2 $3\sigma_g$ orbital and an s,d vanadium hybrid orbital and describes σ donation from dinitrogen to vanadium. This is essentially the same situation found for the $[\text{H}_3\text{VN}_2\text{VH}_3(\mu\text{-Na})]^-$ or $[\text{H}_3\text{VN}_2\text{VH}_3]^{2-}$ complexes. The main difference lies in the singly occupied orbital, which is a $5b_1$ corresponding to an antibonding combination of the $1\pi_u$ of N_2 and the symmetric $d_{xy} + d'_{xy}$ combination of vanadium orbitals (the same situation is found for the $^4\text{A}_1$ state where, however, there are two more singly occupied orbitals, $14a_1$ and $13b_2$, of mainly metallic d character). This feature is confirmed by the increase of the d_{xy} population, which should have otherwise decreased due to back-donation; see Mulliken populations in Table 5. In terms of the M—N—N—M bonding scheme we have that in addition to the completely occupied $1e$ ($3b_1$ and $11a_1$) and $2e$ ($4a_2$ and $12b_2$) orbitals there is one electron in one of the $3e$ orbitals (the $5b_1$). This difference in the bonding picture explains very well the observed geometric effect, as such $3e$ occupancy weakens the V—N bond and strengthens the N—N one.

We will finally consider the $[\text{H}_3\text{VN}_2\text{VH}_3]^{2-}$ complex to confirm that it can be regarded as derived from the $[\text{H}_3\text{VN}_2\text{VH}_3(\mu\text{-Na})]^-$ pulling off the Na^+ ion as already anticipated above. Indeed, an accurate analysis of the Mulliken population and of the molecular orbitals (which is not reported) shows that the bonding picture between dinitrogen and the two VH_3^- fragments in the $^3\text{B}_2$ and $^1\text{A}_1$ states is qualitatively very similar to that found for the corresponding states of the $[\text{H}_3\text{VN}_2\text{VH}_3(\mu\text{-Na})]^-$ complex as discussed above. That discussion can be, therefore, almost exactly repeated with only a renumbering of the MOs (due to the absence of Na^+) and small differences in quantitative composition of the $\sigma(\text{V-N})$, $1e$, and $2e$ orbitals. Moreover, in this case the linearity of the complexes and the absence of the alkali ion make the situation much clear and more similar to the ideal M-N-N-M orbital scheme.

Thermodynamics. When we consider the thermodynamics of the formation of the various complexes there is a certain degree of ambiguity depending on the possible choice of the fragments in the reaction leading to the considered dinitrogen complexes. We choose however the ground state for each considered dinitrogen complex and the simpler possible fragments in the states correlating with it obtaining the following results at CI level (ΔE in kcal mol^{-1}):



The high exothermicity of reaction 1 is essentially due to the electrostatic interaction of the Na^+ ion with the remaining dianionic species, which is in itself unstable as shown by the thermodynamics of reaction 3. However, when we consider the more realistic reaction 2 starting from the sodium atom, in which the electrostatic interaction is correctly counterbalanced by the sodium ionization energy ($119 \text{ kcal mol}^{-1}$), we obtain a more plausible value of $-46 \text{ kcal mol}^{-1}$. On the other hand, reaction 4 shows that dinitrogen is exothermically bonded in the monoanion $[\text{H}_3\text{VN}_2\text{VH}_3]^-$, although for only 8 kcal mol^{-1} .

Note that the N_2 binding energy in these complexes is found to be low (in the $[\text{H}_3\text{VN}_2\text{VH}_3]^-$ case) or even to be due mainly to the stabilization of the alkali ion (in the $[\text{H}_3\text{VN}_2\text{VH}_3(\mu\text{-Na})]^-$ case) in spite of the resulting strongly perturbed structure of the complexed N_2 , a situation very favorable for dinitrogen activation.

The theoretical calculations on the isolated species, while remaining very valuable in understanding the metal- N_2 interactions, the charge distribution, and the activation degree of N_2 , are not very appropriate for justifying the energetics concerning the formation of the above N_2 complexes for a very important aspect. The driving force for the reaction should not be associated with the fragment assembly as reported in eqs 1-4 but rather with the formation and solvation of the counteranions.

Mononuclear Complexes. The formation of the dinuclear vanadium-dinitrogen complexes, **1** and **2**, occurs very probably through the formation of intermediate mononuclear species as discussed in ref 37. This prompted us to extend our calculations to some plausible mononuclear precursors like **7-9**.

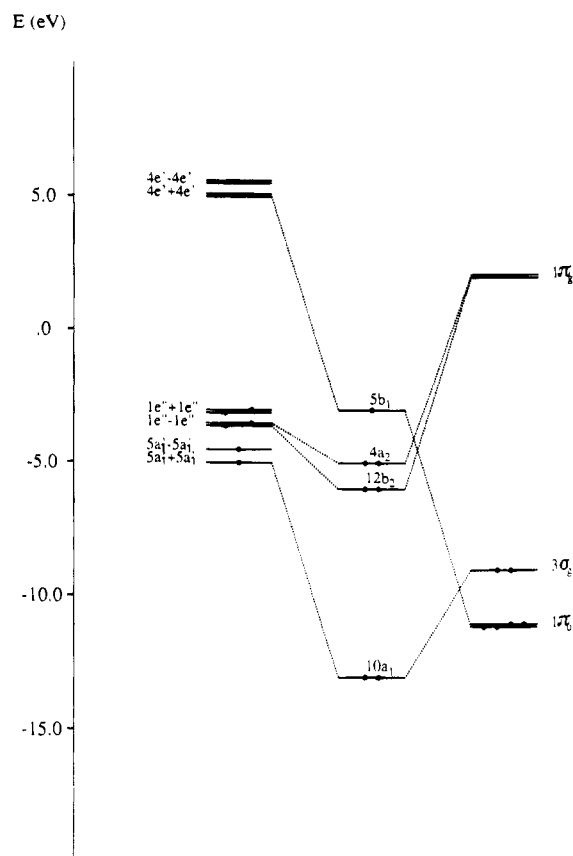


Figure 6. Molecular orbital diagram for the $[\text{H}_3\text{VN}_2\text{VH}_3]^{2-}$ complex in the $^2\text{B}_1$ state.

Table 6. Total SCF and CI Energies (hartree) and Binding Energies (b.e.) (kcal mol^{-1}) for the $[\text{H}_3\text{VN}_2]^-$ and $[\text{H}_3\text{VN}_2\text{Na}]$ Complexes in the Lowest Doublet and Quartet States

	E_{SCF}	E_{CI}	b.e.
$[\text{H}_3\text{VN}_2]^- (^2\text{A}')$	-1053.1274	-1053.6141	+35
$[\text{H}_3\text{VN}_2]^- (^4\text{A}')$	-1053.2095	-1053.6673	+3
$\text{H}_3\text{VN}_2\text{Na} (^2\text{A}')$	-1213.9708	-1214.4584	-70
$\text{H}_3\text{VN}_2\text{Na} (^4\text{A}')$	-1214.0516	-1214.5102	-103

We considered only end-on bonding as this is the geometry correlating with the one observed in the bridging dinuclear complexes we are going to compare and also as end-on bonding is the only geometry observed in stable mononuclear dinitrogen complexes.

The total SCF and CI energies together with the corresponding binding energies for the SCF optimized structures of various states in the end-on configuration are reported in Table 6, while the optimized geometries for the two lowest states are shown in Figure 7. Only data for the $[\text{H}_3\text{VN}_2]^-$ and $[\text{H}_3\text{VN}_2\text{Na}]$ complexes are reported as the neutral $[\text{H}_3\text{VN}_2]$ species is not stable. From these data we see that the ground state is a quartet in both the $[\text{H}_3\text{VN}_2]^-$ and $[\text{H}_3\text{VN}_2\text{Na}]$ species and that dinitrogen is slightly nonbonding ($+3 \text{ kcal mol}^{-1}$ at the CI level) in the $[\text{H}_3\text{VN}_2]^-$ species and is strongly bonding ($-103 \text{ kcal mol}^{-1}$ at the CI level) in the $[\text{H}_3\text{VN}_2\text{Na}]$ one. However, we must consider that the high value for the $[\text{H}_3\text{VN}_2\text{Na}]$ case is mainly due to the electrostatic interaction between Na^+ and the $[\text{H}_3\text{VN}_2]^-$ fragments which constitute its structural units, as shown below, so that accounting for the sodium ionization energy ($119 \text{ kcal mol}^{-1}$) N_2 is slightly not bonding also in this latter case.

Considering first the simpler $[\text{H}_3\text{VN}_2]^-$ complex, we see that in the doublet state the bonding structure can be interpreted in terms of the Chatt-Dewar-Duncanson model with minor

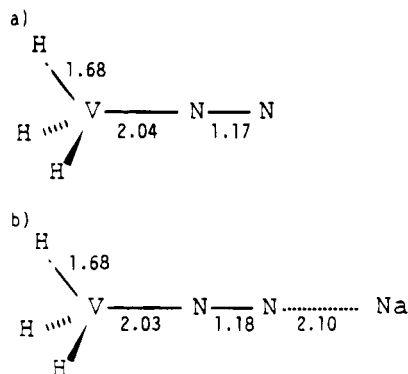


Figure 7. Optimized geometries of the (a) $[\text{H}_3\text{VN}_2]^-$ and (b) $[\text{H}_3\text{VN}_2\text{-Na}]$ complexes both in the $^4\text{A}'$ state.

modifications due to the extra negative charge and to the open shell nature. Indeed, the analysis of the molecular orbitals shows that the main bonding orbitals between vanadium and dinitrogen are the highest doubly occupied $4a''$ and the singly occupied $16a'$, which can be viewed as the overlap between the occupied vanadium $3d_{yz}$ and the z component of the virtual $1\pi_g$ orbital of N_2 and between the occupied vanadium $3d_{xy}$ and the x component of the virtual $1\pi_g$ orbital of N_2 , respectively. Although both these orbitals describe π back-donation from vanadium to dinitrogen, it is worth noting that the first one is mainly of metallic character while the second one is mainly of dinitrogen character so that dinitrogen is not much activated and supports most of the spin population (0.89). σ donation is described by the $12a'$ orbital which represents the overlap between the 3σ orbital of dinitrogen and an hybrid vanadium orbital, formed mainly by $4s$ and $4p_y$. This description is confirmed by the analysis of the Mulliken population changes and leads to the diagram of the highest energy levels with the corresponding interactions between the MOs of the VH_3^- and N_2 fragments reported in Figure 8.

Passing to the quartet state, we found a fairly similar situation, with one of the two MOs describing π back-donation, the singly occupied $6a''$ one, with more metallic character (the other two singly occupied ones being essentially constituted by pure metal d orbitals). The more relevant difference with the doublet state is therefore the weaker V—N bond as indicated also by the longer V—N distance (2.04 Å versus 1.98 Å for the doublet).

When we consider the $[\text{H}_3\text{VN}_2\text{Na}]$ complex, the analysis of the atomic Mulliken populations shows an atomic charge of +0.92 e on the sodium, which clearly indicates that such complex is constituted of a Na^+ ion and a $[\text{H}_3\text{VN}_2]^-$ unit. This fact is confirmed by the analysis of the highest molecular orbitals which are almost identical (same energy ordering and qualitatively similar compositions) to those of the $[\text{H}_3\text{VN}_2]^-$ complex, in both the doublet and quartet states, so that the $[\text{H}_3\text{VN}_2\text{Na}]$ complex presents essentially the same bonding picture of the $[\text{H}_3\text{VN}_2]^-$ unit in the corresponding states.

Altogether, the results discussed above indicate a fairly poor perturbation of the dinitrogen molecule (N—N distances of 1.18 and 1.17 Å, respectively, for the complexes with and without Na) caused by an essentially single occupation of the dinitrogen antibonding $1\pi_g$ orbitals only slightly mixed with metal d orbitals and a weak V—N bond (cf. the V—N distances of 2.03 and 2.04 Å) mainly due to σ donation. Moreover the binding energies obtained show that these complexes are essentially very slightly unstable (at most a few kcal mol^{-1}) or thermoneutral. This result supports the hypothesis of the not isolable species **8** and **9** as intermediates in the formation of complex **6**. It also

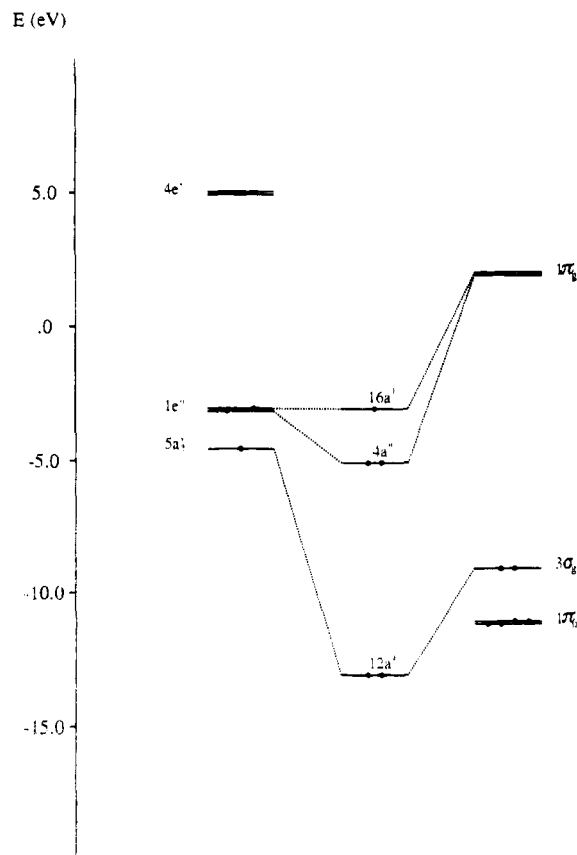


Figure 8. Molecular orbital diagram for the $[\text{H}_3\text{VN}_2]^-$ complex in the $^2\text{A}'$ state.

explains the unsuccessful trials to isolate mononuclear dinitrogen complexes of vanadium(II) and vanadium(III).

Conclusions

This study at the *ab initio* RHF and CI level has shown that dinitrogen is (i) bonded and strongly activated in the $[\text{H}_3\text{VN}_2\text{-VH}_3(\mu\text{-Na})]^-$ and $[\text{H}_3\text{VN}_2\text{VH}_3]^{2-}$ complexes of V(II)-V(II) character, (ii) bonded and perturbed, although to a lesser extent, in the $[\text{H}_3\text{VN}_2\text{VH}_3]^-$ complex of V(II)-V(III) character, and (iii) neither bonded nor perturbed in the $[\text{H}_3\text{VN}_2\text{VH}_3]$ complex of V(III)-V(III) character. This shows a strong dependence of the dinitrogen activation in the considered dinuclear complexes on the oxidation states of the two vanadium centers with a decrease of the activation passing from V(II) to V(III). Moreover the peculiar magnetic behavior of these complexes can be explained as due to a quasi-degeneracy of the higher mono-electronic levels, corresponding to nonbonding $d-d$ and slightly bonding $d-\pi^*$ interactions, whose order depends critically on the vanadium oxidation state. The analogous calculations performed on the mononuclear $[\text{H}_3\text{VN}_2\text{Na}]$, $[\text{H}_3\text{VN}_2]^-$, and $[\text{H}_3\text{VN}_2]$ complexes, of V(III) and V(II) character, have shown an almost negligible activation in the V(II) case only, ruling out a real mononuclear dinitrogen activation by V(II) or V(III) complexes.

Acknowledgment. The present work has been carried out within the "Progetto finalizzato CNR Materiali Speciali per Tecnologie Avanzate". The authors thank the CINECA for providing a computer grant. Thanks are due to the IBM Semea for providing a fellowship to one of us (N.R.) in the framework of a joint study. Support by the Fond Nazionale Suisse de la Recherche Scientifique and the COST 03 Action is gratefully acknowledged.